Analytical study of the waste heat in a Hygroscopic Cycle with high lithium bromide concentration for energy use

Roberto Martínez-Pérez[a], Andrés Meana-Fernández[a],
Juan Manuel González-Caballín[a], Alessia Manfredi[b],
Francisco Javier Rubio-Serrano[c] and Antonio José Gutiérrez-Trashorras[a]

[a] *Department of Energy - University of Oviedo, Gijón, Spain, martinezroberto@uniovi.es (CA),*
andresmf@uniovi.es, gonzalezsjuan@uniovi.es, gutierrezantonio@uniovi.es
[b] *Department of Industrial Engineering - University of Padua, Padua, Italy, alessia.manfredi.1@phd.unipd.it*
[c] *Imasa Technologies S.L.U. (Imatech), Madrid, Spain, fj.rubio@imasatechnologies.com*

Abstract:

The current world energy context requires solutions to reduce energy demand and increase the energy efficiency of thermal power plants, which typically release heat into the ambient without a further useful purpose. Climate change, leading to higher temperatures and water scarcity, may make difficult heat rejection processes in power cycles. Hygroscopic Cycle Technology can become a relevant technology due to the increase in the cooling reflux temperature thanks to the incorporation of hygroscopic salts. This work analyzes the possibility of using the waste heat rejected from the cycle cooling reflux by developing a thermodynamic model with a lithium bromide-water (LiBr-H_2O) mixture as the working fluid. The model, validated with experimental tests performed at a pilot plant, was used to optimize cycle operating conditions regarding waste heat recovery potential without substantially decreasing the cycle efficiency. The increase in LiBr mass concentration led to higher cooling reflux temperatures, allowing for easier heat rejection and an increase in enthalpy and the cooling reflux mass flow rate. The effect of condensing pressure was found to have a relatively low impact on the mass flow rate and the potential heat recovery per unit mass flow. An exergy analysis revealed a decrease in potential physical exergy recovery as LiBr concentration increases. Concentrations between 30 and 50% seem the most suitable ones for maximizing the power output of the cycle, while maintaining a high enough heat recovery potential, with values of 0.6 kJ/kg for the optimum concentration of 45%. Finally, prospective uses for the waste heat are proposed, considering that current applications of the technology rely on the use of biomass fuels from olive oil production waste.

Keywords:
Cycle Optimization; Hygroscopic Cycle Technology; Thermodynamic Modelling; Waste Heat Recovery Potential.

1. Introduction

Current environmental conditions and resource depletion trends are a worldwide challenge. In this context, electricity and heat generation represent the primary source of CO_2 emissions, reaching an all-time high of 14.6 Gt in 2022 [1]. Furthermore, electrical generation accounted for approximately 20% of global final energy consumption in 2021, with renewables contributing in 28% [2]. Moreover, the increasing electrification of the energy system and the growing population result in scenarios with significant increments in energy demand [2], requiring greater power generation capacities [3] while aiming for decarbonization and energy transition [4]. For this purpose, the Paris Agreement [5] aims for net-zero emissions by 2050 to prevent further rising of ambient temperatures and freshwater scarcity. In this sense, power generation, accounting for around 15% of freshwater withdrawal [6], plays a vital role, as the supply shortfall is expected to reach 40% by 2030 [7], while water consumption in the energy sector is predicted to rise 50% [8]. In this regard, energy supply reliability may be affected by droughts, as water stress hinders thermodynamic power cycles, which are key for the generation mix. Recent water shortage episodes have led to shutdowns and output disruptions. For instance, in France, the Chooz nuclear power plant was interrupted for two months in 2020 [2]. It is also estimated that India lost 14 TWh of thermal power generation in 2016 due to water shortfall [9]. In addition, rising ambient temperatures also lead to lower efficiencies of condensing and cooling systems, resulting in thermal processes being unable to respect discharge water temperature regulations. Lack of freshwater resources may also become problematic, with more significant desalination needs leading to greater energy demand. Hence, the viability of thermodynamic power cycles depends strongly on developing water-smart processes with

advanced cooling systems [8]. Ultimately, economic dependence on energy [10] and primary sources implies profound strategic and social implications. In this sense, stress over resources affects energy security [11], not only in reliability, stability and availability terms but also in affordability, with electricity rate increments [12], jeopardizing proper development of manufacturing industries, services and commodities. In this regard, worldwide policies are gradually turning towards sustainability through non-linear production and consumption models. Subsequently, circular economy [13] stands as the economic paradigm to minimize waste and pollution by extending the life cycle of products through reusing and recycling strategies in order to protect natural assets while ensuring secure and affordable energy supplies.

As per the state of the art, thermal efficiency and saving upgrade research has been intensely focused on recovering waste heat. Early analysis evaluated the introduction of regenerative-reheat processes within the Rankine cycle showing thermal efficiency increments of up to 14% [14]. Moreover, Tuantuan et al. [15] proposed a method for re-heat and regeneration stages optimization. Additional Rankine process stages have been further evaluated. In [16], the impact of close Feed-Water Heaters (FHWs) on the efficiency of a 200 MWe power plant was performed, resulting in a maximum efficiency enhancement of 10%. External source heat integration for water pre-heating has also been considered in the literature. Hu et al. [17] introduced the concept of Solar Aided Power Generation (SAPG) by replacing turbine steam bleed-offs for FWHs in regenerative Rankine with solar thermal energy. Prosin et al. [18] proposed a thermal power plant configuration in which secondary air flux was to be heated by solar thermal energy. Furthermore, Nsanzubuhoro et al. [19] considered geothermal energy as Low-Pressure Feed-Water Heaters (LPFHs) source. Solar thermal energy inclusion has been further evaluated. In this sense, Li et al. [20] examine the performance of Rankine cycles with a solar double re-heat system, observing a significant reduction in fuel consumption.

As energy demand grows, development has focused on cycles capable of operating with low-grade heat sources, which were technically unfeasible with previous systems [21]. In this regard, the Organic Rankine Cycle (ORC), Goswami Cycle (GC) and Kalina Cycle (KC) represent the most notorious power generation systems developed to work with low-grade temperature inputs [22], such as geothermal, solar thermal, waste heat and biomass combustion, by basing their operation on working fluids with boiling points lower than pure water. To date, most of the research efforts have concentrated on ORC, as it presents higher efficiency levels than those of GC and KC, which, although normally ranging between 10% and 18%, can reach peaks of up to 30% depending on the cycle parameters [22]. Moreover, ORC is generally more cost-effective due to its lower complexity and, consequently, lower capital and maintenance costs [23]. Additionally, ORCs can be easily adapted to a wide range of heat sources [24] and working fluids [25] while offering greater reliability due to its deeper study. Instead of rejecting heat into the environment, Combined Heat and Power (CHP) systems pose as an alternative for taking advantage of waste heat from power generation processes for practical applications, increasing thermal efficiency. As an example, Ballzus et al. [26] presented the Hellisheiði geothermal plant, which produces electricity (303 MWe) and hot water (133 MWt) for district heating [27] by harnessing thermal energy from the turbine exhaust steam.

Prevailing energy challenges require bold technical improvements in thermodynamic power systems to guarantee supply. In this context, the Hygroscopic Cycle Technology (HCT) [28], first developed in 2010 by Imatech, opens new prospects toward long-term power generation sustainability, posing as a Rankine cycle enhancement regarding efficiency, condensing and cooling terms. For this purpose, HCT operates with mixtures of water and hygroscopic compounds [29] as the working fluid, enabling to condensate turbine exhaust steam through absorption phenomena. As a result, HCT can optimize overall performance by working at lower condensing pressures for a given condensing temperature, effectively increasing the electrical power output of the cycle. Furthermore, absorption through hygroscopic compounds displays higher condensing temperatures [30], enabling the adoption of dry-cooling systems. In this sense, HCT can reject heat more efficiently, allowing the cycle to operate at high ambient temperatures, even over 45 ºC. Dry mode refrigeration advantages further expand as HCT is able to fully decouple power generation from water withdrawal, consequently expanding power plant availability while eliminating steam emissions. Low-concentration HCT has already been developed at an industrial scale. For example, HCT was implemented in Vetejar 12.5 MWe biomass power plant [31], successfully extending availability as the cycle was decoupled from disadvantageous climate conditions due to high external temperatures and water scarcity. Findings showed a 100% cooling water savings of 229,200 m^3/year, an additional 75 MWh/month power generation and a 150 MWh/month reduction of self-consumption due to high-efficiency dry-coolers. Other cases [28] like Baena 25 MWe biomass power plant and Industrias Doy 4.5 MWe cogeneration facilities emphasize the potential of HCT as it can be adapted [32] to any power generation range.

Despite the above improvements, HCT is subject to further enhancement, especially considering thermodynamic power cycles adaptation requirements toward circular economy principles and, subsequently, environmental protection [33]. In this sense, thermal efficiency improvement within HCT becomes relevant, especially with high hygroscopic concentrations where the thermal grade of the condensate flux is greater.

Currently, there are no HCT plants with implemented waste heat recovery systems. In this context, the work presented in this manuscript aims to evaluate the potential for waste heat recovery in high-concentration lithium bromide HCT (HC-HCT). With this objective, a thermodynamic model for evaluating the potential of waste heat recovery has been developed and validated with experimental tests. The final objective is to optimize operating conditions of the cycle regarding waste heat recovery potential without substantially decreasing the cycle efficiency. In addition, prospective uses for the waste heat are proposed, considering that current applications of HCT rely on the use of biomass fuels from olive oil production waste.

2. Methodology

To fulfill the objectives of this study, experimental tests were performed in the HCT pilot plant developed by Imatech in Gijón (Spain) to characterize the thermodynamic conditions at the condensing and cooling systems with high hygroscopic concentration. Then, the results were used to validate an analytical model capable of estimating the potential for the recovery of HCT waste heat.

2.1. Experimental methodology

The HCT pilot plant developed by Imatech in Gijón (Spain), used for performing the experimental tests of this work, is presented in Figure 1. In this work, the hygroscopic salt used is lithium bromide (LiBr) due to its several advantages: LiBr is highly hygroscopic but easily desorbed from water, non-flammable, non-toxic and chemically stable at typical cycle operating conditions.
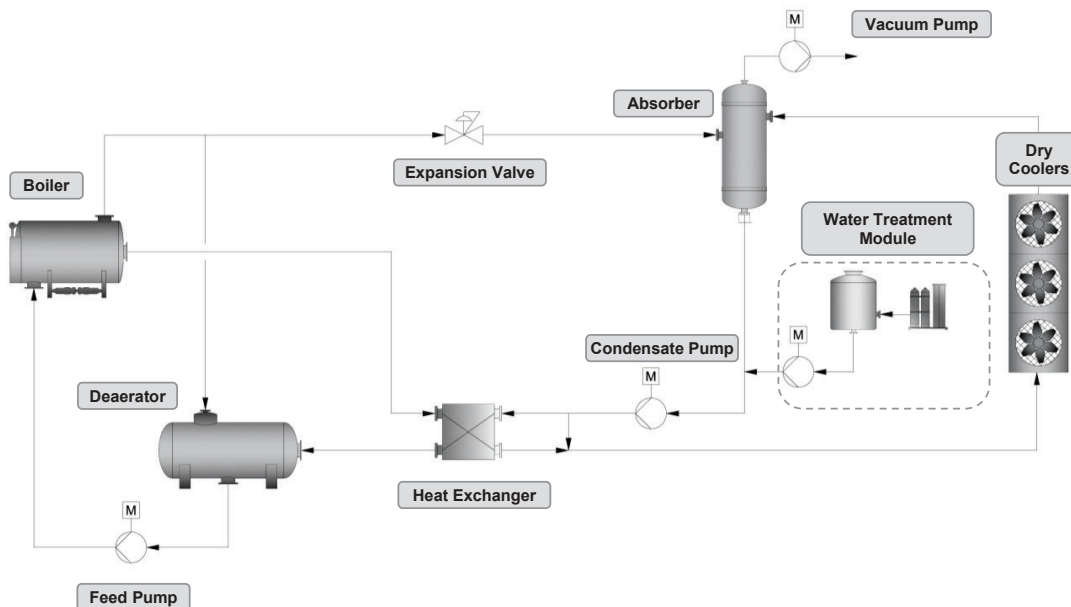

Figure 1. Operation process of HCT pilot plant.

The pilot plant is able to reproduce HCT power plant conditions by generating 100 kg/s of superheated steam at 14 bar and a maximum temperature of 200ºC. This steam is then led to an expansion valve that simulates the behavior of a 30 kW turbine-generator. The valve outlet steam then flows to the absorber, the key component of the HCT. In the absorber, the steam is condensed by absorbing a high-concentrated LiBr/H_2O cooling reflux coming from the dry cooling system that enters the absorber through nozzles to increase contact surface. Condensing pressure is controlled using a vacuum pump. The condensate then leaves the absorber, is pumped by the condensate pump and is separated into two flows: one continues to the boiler, while the other one is recirculated towards the dry coolers, releasing heat from the cycle, to be later reinjected into the absorber to provide the required salts for absorption to take place. A closed heat exchanger is used to recover thermal energy from boiler blowdowns to pre-heat the condensate water, which is then sent to a deaerator before entering the boiler, where LiBr salts are desorbed and purged. LiBr-H_2O mixtures are prepared and controlled via a 2 m^3 atmospheric tank and a demineralizing water module. Concentration values are derived from electrical conductivity measurements from samples taken from cycle purges.

The instrumentation used for performing the experiments is collected in Table 1. Data were collected using a Supervisory Control and Data Acquisition (SCADA) system developed by Siemens (SIMATIC S7, maximum uncertainty 0.004%).

Table 1. HCT pilot plant instrumentation.

Parameter	Instrument	Accuracy
Temperature	Endress+Haussser TR-61 platinum resistances PT100 RTD	± 0.1 °C
Absolute pressure	Aplisens PCE-28	± 0.5 %
Mass flow	Khrone OPTISWIRL-5080	± 0.5 %
Electrical conductivity	HANNA HI 98188-02	± 2.0 %

The parameters set for the different tests are collected in Table 2.

Table 2. HCT pilot plant working parameters.

Parameter	Value
Steam mass flow ($\dot{m}_S$)	100 kg/h
Steam temperature (T_S)	170 °C
Condensing pressure (P_C)	3, 5, 7, 10, 15 kPa
LiBr concentration at the condensate (C_C)	45 %
Ambient temperature (T_C)	15 °C
Temperature drop at dry coolers (ΔT_{DC})	7 °C

2.2. Analytical model

2.2.1. Description of the model

Engineering Equation Software (EES, version V10.833-3D) [34] was used to develop a thermodynamic model of the condensing and cooling process of the HC-HCT, as represented in the scheme of Figure 2. The range of condensing pressure (P_C) studied was from 1 to 20 kPa.
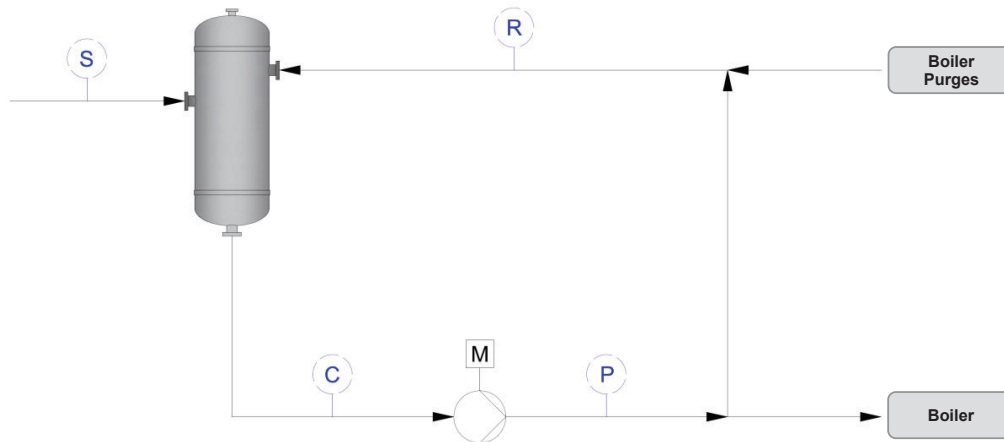

Figure 2. HCT condensing and cooling process model detail.

The following assumptions were considered to develop the model: kinetic and potential energy changes are negligible; the condensate pump only compensates for pressure losses in the pipes and equipment, which are perfectly insulated; and, since the cycle is closed, only the physical exergy is considered to estimate waste heat potential. The condensing process in the absorber is described by the mass, concentration and energy balances in Eqs. (1-3):

$$\dot{m}_S + \dot{m}_R = \dot{m}_C \tag{1}$$
$$\dot{m}_S \cdot C_S + \dot{m}_R \cdot C_R = \dot{m}_C \cdot C_C \tag{2}$$
$$\dot{m}_S \cdot h_s + \dot{m}_R \cdot h_R - \dot{Q}_D = \dot{m}_C \cdot h_C \tag{3}$$

The thermal power from the heat of dilution $\left(\dot{Q}_D\right)$ depends on the difference between the concentration of the condensate (C_C) and reflux (C_R) streams. In this case, the correlations proposed by Yuan and Herold [35] were

implemented into the model. The LiBr concentration at the turbine outlet (C_S) was set to zero, being pure steam. The thermodynamic state at the condensate pump outlet was obtained from the isentropic efficiency of the pump (η_{CP}), considered 50%, according to industrial values from small centrifugal pumps [36]. Eqs. (4) and (5) determine the pump outlet properties:

$$\dot{m}_C = \dot{m}_P \tag{4}$$

$$\eta_{CP} = \frac{h_{Ps} - h_C}{h_P - h_C} \tag{5}$$

Once the energy analysis of the condensing and cooling process was finished, the physical exergy recovery potential (ex_{RCVY}) from the cycle cooling process was estimated with Eq. (6) as the difference between the physical exergy per unit mass of the flow before (ex_P) and after (ex_R) the heat rejection process, calculated with Eq. (7) [37]:

$$ex_{RCVY} = ex_P - ex_R \tag{6}$$

$$ex_i = (h_i - h_\infty) - T_\infty(s_i - s_\infty) \tag{7}$$

The reference environment or dead state for the exergy calculations was defined accordingly to the methodology proposed in [38]. The dead state temperature was set as the mean ambient temperature during the experimental tests, T_∞=15 ºC. The overall mass and volume of the cycle are constant, so no pressure equilibrium can be achieved with the exterior. Hence, the dead state pressure was set to the condensing pressure. The composition of the dead state was calculated at chemical equilibrium within the cycle, with the chemical potential of water in the LiBr-H_2O solution matching the Gibbs free energy of the water vapor, resulting in 0% of LiBr mass concentration for all the considered pressure values (over 1 kPa).

Finally, the heat per unit mass of cooling reflux rejected to the environment was corrected with the Carnot factor to study the influence of ambient temperature in the process, defined as:

$$\theta_{CP} = 1 - \frac{T_\infty}{T_{HR}} \tag{8}$$

With the temperature at which the fluid rejects heat (T_{HR}) calculated as the logarithmic mean between the temperatures of the condensate pump outlet (T_P) and the cooling reflux (T_R) [27]:

$$T_{HR} = 1 - \frac{T_P - T_R}{log\left(\frac{T_P}{T_R}\right)} \tag{9}$$

2.2.2. Experimental validation

Figure 3a shows the condensate and cooling reflux mass flow rates calculated by the model alongside the experimental measured values for 45% LiBr concentration. It may be appreciated that the developed models are able to follow the tendency of the experimental results, with a slight underprediction in the mass flow rates that increases with the condensing pressure up to a maximum error of 3%.

Regarding the prediction of enthalpy values, Figure 3b depicts the contrast of the model with experimental results. The tendency of the evolution of enthalpy values with the condensing pressure is adequately followed by the model, with average errors of 5%. Therefore, the developed model may be considered as suitable for the analysis of the thermodynamic processes of the cycle under study.
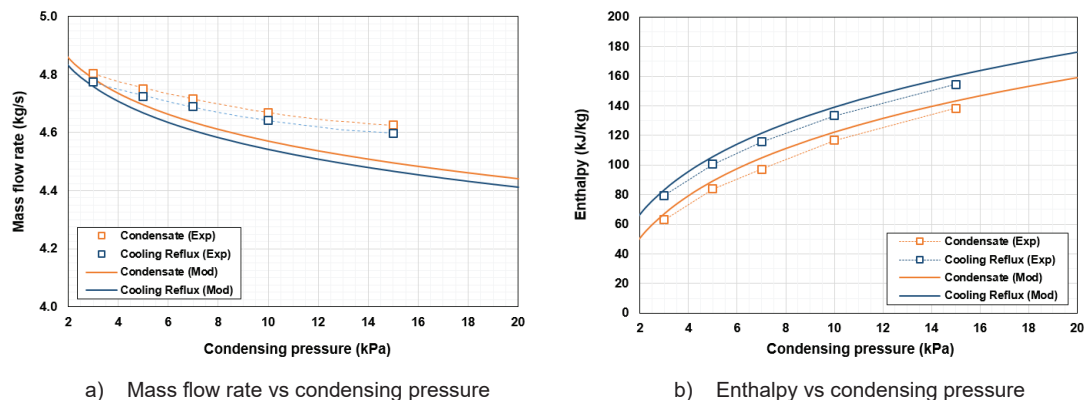

a) Mass flow rate vs condensing pressure   b) Enthalpy vs condensing pressure

Figure 3. Experimental validation of the model

3. Results

Firstly, the results of the thermodynamic parametric analysis of the model are presented. Then, the selection of the most suitable operating conditions for the cycle are discussed and potential applications for the recovery of heat waste form the cycle are presented.

3.1. Thermodynamic parametric analysis

Figure 4 shows the evolution of the condensate temperature as a function of the LiBr concentration of the reflux and the condensing pressure. It may be observed that the increase in concentration leads to higher temperatures, with a slower increasing rate up to 30% LiBr concentration.

Above this concentration value, the slope of the temperature curves becomes much greater. The increase in pressure has an additional effect of increasing condensing temperature. The increase of the condensate temperature may be linked to higher temperature differences with the environment and thus an easier heat rejection from the cycle and possibly easier use of that waste energy. Nevertheless, it must be considered that, if the turbine power is kept constant and the heat rejected increases, more fuel consumption at the boiler will be required. Paralelly, if the heat input at the boiler is kept constant and the heat rejected increases, there will be less power delivered by the turbine and the cycle efficiency will decrease.
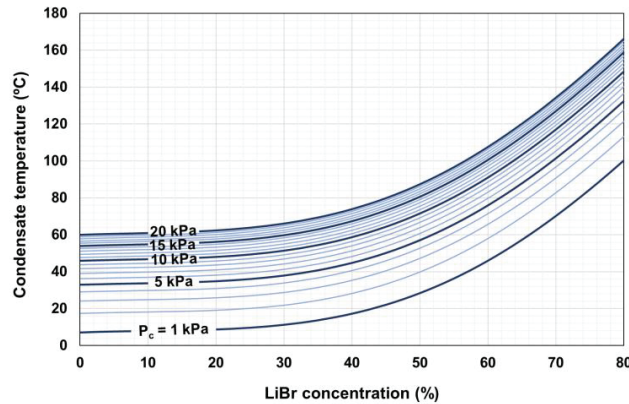
Figure 4. Condensate temperature as a function of LiBr concentration and condensing pressure

The results from the change of enthalpy with respect to LiBr concentration and condensing pressure are shown in Figure 5. A minimum for all curves may be found around 45% LiBr concentration, hinting to the selection of this concentration to minimize the enthalpy difference at the turbine and thus maximize the power delivered by the cycle. With concentration values up from this point, the condensate enthalpy increases very quickly, discouraging too high concentration values for the optimal performance of the turbine. Regarding the condensing pressure, it should be kept as lower as possible if the aim is to maximize cycle efficiency.
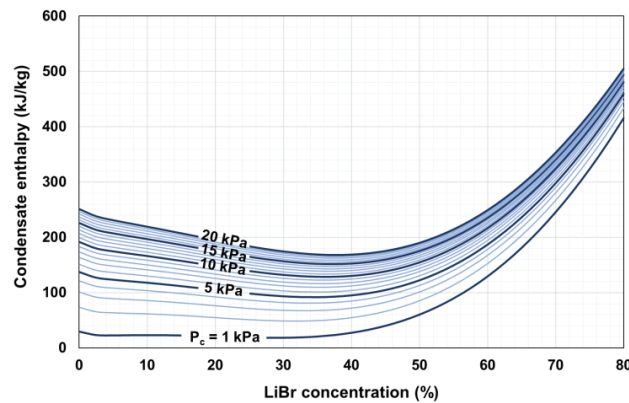
Figure 5. Condensate enthalpy as a function of LiBr concentration and condensing pressure

The cooling reflux mass flow rate shows an increasing trend with the increase of LiBr concentration, as shown in Figure 6. The effect of pressure in the ranges studied does not have a determining effect, becoming more important at intermediate LiBr concentration values. Nevertheless, for the sake of clarity, the results of all the pressure values studied have been averaged and represented as intervals with a 95% confidence level. It may be observed that the cooling reflux mass flow rate increases with the concentration, requiring a higher working fluid consumption and potentially leading to higher pumping requirements and pressure losses in the circuit. It seems sensible to keep the values of LiBr concentration below 50%, to avoid the steeper increase in the mass flow rate that comes with the increase of concentration.
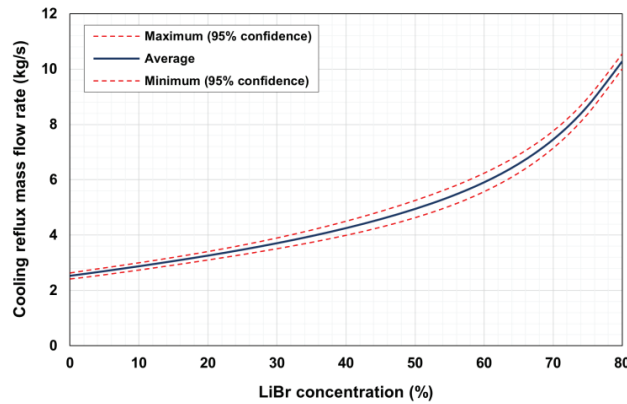

Figure 6. Average cooling reflux mass flow rate as a function of LiBr concentration

Regarding the heat recovery potential per unit mass of the cooling reflux, Figure 7 shows the results from the energy balance. Again, the effect of the pressure only becomes noticeable for intermediate LiBr concentration values, but it is minimal compared with the effect of LiBr concentration, so the values have been averaged and represented again as intervals with a 95% confidence level. A decreasing trend in the heat per unit mass is observed as the LiBr concentration increases, probably due to the increasing mass flows in the cycle. From these results, it seems sensible to try to maximize the heat per unit mass and avoid too high LiBr concentration values, which results in a lower energy density for potential applications.
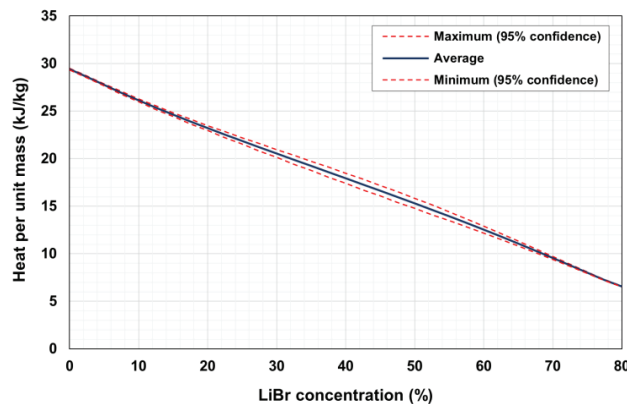

Figure 7. Heat recovery potential per unit mass of cooling reflux as a function of LiBr concentration

Finally, to evaluate the feasibility of the heat recovery process itself, the results from the physical exergy recovery potential per unit mass of cooling reflux mass flow, considering the dead state from the experimental conditions, are presented in Figure 8. In this case, the role of the condensing pressure cannot be overlooked, with higher condensing pressures leading to higher exergy recovery potentials. For the lowest condensing pressures, below 2 kPa, physical exergy increases with the increase in concentration. The negative values of potential recovery at these pressure conditions may be ascribed to the fact that the temperatures at the absorber would become lower than the dead state temperature. In addition, these lower pressures require higher-performance vacuum pumps, so there is no apparent reason to work at these operating conditions.

On the other hand, the global trend with the increase of LiBr concentration is the decrease of the potential specific exergy recovery. This decrease becomes more apparent for LiBr concentrations above 50%,

discouraging again the use of too high concentration values. The region between 30 and 40% shows a relatively smooth decrease with the increase in concentration, with similar potential recovery values. This advantage could be exploited for the stable operation of the heat recovery system.
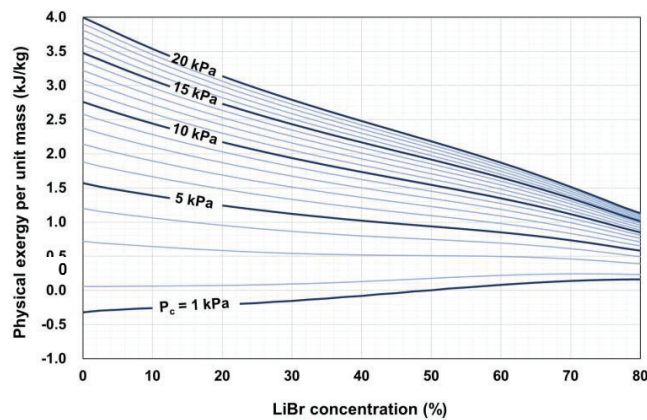

Figure 8. Physical exergy recovery potential per unit mass as a function of LiBr concentration

In summary, gathering all the results from the parametric analysis, it may be proposed to use concentrations of LiBr around 45% to maximize the enthalpy difference at the turbine. The exergy analysis has revealed that, at the dead state conditions of the experiment, the physical exergy recovery potential per unit mass of cooling reflux decreases sharply for values above 60%. On the other hand, concentration values lower than 30% may not achieve cooling reflux temperatures high enough for cycle heat rejection.

Regarding pressure values, selecting 5 kPa as the condensing operating pressure has several advantages. It increases the pressure difference at the turbine with respect to higher operating pressures, resulting in a higher turbine power output and in cooling reflux temperatures high enough to release heat from the cycle. In addition, it does not result in a significant effect regarding the cycle mass flow rates or the actual energy recovery potential per unit mass of cooling reflux. Apart from requiring higher-performance vacuum pumps, lower pressures are not justified in terms of the exergy analysis, while an operating pressure of 5 kPa has been verified in actual power plant operation.

3.2. Potential applications of waste heat recovery

After selecting a pressure of 5 kPa as the condensing pressure and 45% as the LiBr concentration for cycle waste heat recovery, the effect of the ambient temperature in the heat recovery potential per cooling reflux unit mass is depicted in Figure 9, to evaluate possible applications for the recovered waste heat.
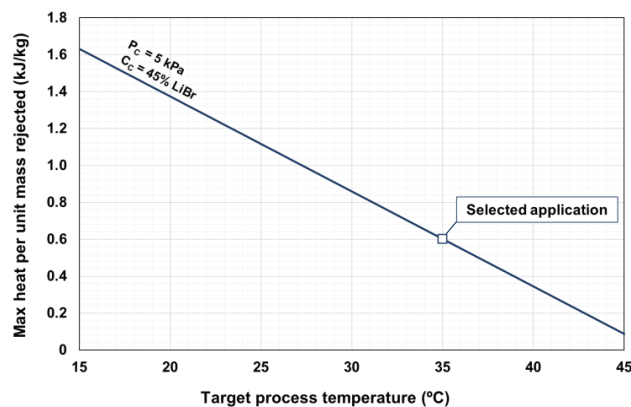

Figure 9. Heat recovery potential per cooling reflux unit mass vs ambient temperature.

Although desirable, it is not possible to reach conditions for pyrolysis (250ºC) or alperujo drying (100ºC) to treat the biomass and use it in the cycle boiler [39]. Nevertheless, there is enough potential for developing anaerobic mesophilic processes at 35ºC for biogas production [40] or compost for agriculture [41] with a

potential heat recovery of 0.6017 kJ/kg of cooling reflux. Considering typical industrial cooling reflux values of around 6000 t/h in HCT cycles, the potential heat that could be delivered to the biodigesters is in the range of 1 MW.

4. Conclusions

The current world energy context requires solutions to reduce energy demand and increase the energy efficiency of power plants. Thermal power plants typically release heat into the ambient without a further useful purpose. Climate change, leading to higher temperatures and water scarcity, may difficult heat rejection processes in power cycles. HCT can become a relevant technology due to the increase in the temperatures in the cooling reflux produced by the incorporation of hygroscopic salts, such as LiBr. In this work, it has been possible to analyze the possibility of using the waste heat rejected from the cooling reflux of the HCT by developing a thermodynamic model in EES and validating it with experimental tests. The main conclusions obtained are collected in the following paragraphs.

Firstly, the results from the thermodynamic parametrical analysis have revealed that the increase of LiBr leads to higher temperatures in the cooling reflux. This may be linked to easier heat rejection to the environment and thus an easier use of that waste energy, but the effect on the power delivered by the cycle and its thermal efficiency must also be considered. Regarding the enthalpy at the absorber outlet, a minimum value, linked to higher cycle power output values, was found to be around 45% LiBr concentration. With the increase of LiBr concentration up from this point, this enthalpy and the cooling reflux mass flow rate showed a steep increase trend. As these higher mass flow rates lead to higher pumping requirements and pressure losses in the pipes and equipment, values of LiBr concentration over 60% are strongly discouraged. On the other hand, the effect of condensing pressure was relatively small to the effect of LiBr concentration in both the mass flow of the cooling reflux and the heat recovery potential per unit mass of the cooling reflux. The increase of LiBr concentration was also linked to a decreasing trend in the heat recovery potential per unit mass and a lower energy density for potential applications.

The exergy analysis of the cooling process revealed a decrease in the potential physical exergy recovery with the increase of LiBr concentration, becoming more apparent with concentrations above 50%. Considering all the results obtained from this work, concentrations of LiBr around 45% seem the most suitable ones for maximizing the power output of the cycle, always working in the range between 30 and 50%. Regarding pressure values, 5 kPa of condensing pressure seems promising, finding a compromise between the pressure difference at the turbine and temperature high enough for heat rejection in the cooling reflux.

Finally, the results of evaluating the cycle with 45% LiBr concentration and a condensing pressure of 5 kPa for different ambient temperatures resulted in the identification of potential applications for the cycle. Sadly, pyrolysis or alperujo drying temperatures cannot be reached with this cycle configuration, preventing the use of this heat to treat olive residue as fuel in the biomass boiler of the circuit. Nevertheless, there is enough potential for developing anaerobic mesophilic processes at 35ºC for the production of biogas or compost for agriculture, with a potential heat recovery of 0.6017 kJ/kg of cooling reflux.

Acknowledgments

Nomenclature

C	mass concentration, %
ex	physical exergy per unit mass, kJ/kg
h	enthalpy per unit mas, kJ/kg
$\dot{m}$	mass flow rate, kg/s
P	absolute pressure, kPa
Q	heat, kW
T	Temperature, ºC

Greek symbols

η	efficiency, %
θ	Carnot factor, %

Subscripts and superscripts

C	condensate
CP	Condensate pump
DC	dry cooler
HR	recovery heat
P	condensate pump outlet
R	cooling reflux
$RCVY$	recovery
S	steam
∞	dead state

References

[1] International Energy Agency (IEA), "CO2 Emissions in 2022," 2022. Accessed: Mar. 01, 2023. [Online]. Available: https://www.iea.org/reports/co2-emissions-in-2022

[2] International Energy Agency (IEA), "World Energy Outlook 2022," 2022. Accessed: Mar. 01, 2023. [Online]. Available: https://www.iea.org/reports/world-energy-outlook-2022

[3] BP plc, "Statistical Review of World Energy 2021," 2021. Accessed: Mar. 01, 2023. [Online]. Available: https://www.bp.com/en/global/corporate/energy-economics/energy-outlook.html

[4] International Energy Agency, "Net Zero by 2050 - A Roadmap for the Global Energy Sector," 2021. Accessed: Mar. 01, 2023. [Online]. Available: https://www.iea.org/reports/net-zero-by-2050

[5] United Nations (U.N.), "Conference of the Parties, Adoption of the Paris Agreement." United Nations (U.N.), 2015. Accessed: Mar. 01, 2023. [Online]. Available: https://treaties.un.org/Pages/ViewDetails.aspx?src=IND&mtdsg_no=XXVII-7-d&chapter=27&clang=_en

[6] J. C. Terrapon-Pfaff, W. Ortiz, P. Viebahn, E. Kynast, and M. Flörke, "Water Demand Scenarios for Electricity Generation at the Global and Regional Levels," *Water (Switzerland)*, vol. 12, no. 9, Sep. 2020, doi: 10.3390/w12092482.

[7] United Nations Environmental Program (UNEP), *Options for Decoupling Economic Growth from Water Use and Water Pollution*. 2016. Accessed: Mar. 01, 2023. [Online]. Available: https://wedocs.unep.org/handle/20.500.11822/7539;jsessionid=E1936BD6383E87C738483E8B592A8DF3

[8] International Energy Agency (IEA), "If The Energy Sector Is To Tackle Climate Change, It Must Also Think About Water," 2020. Accessed: Mar. 01, 2023. [Online]. Available: https://www.iea.org/commentaries/if-the-energy-sector-is-to-tackle-climate-change-it-must-also-think-about-water

[9] T. Luo, D. Krishnan, and S. Sen, "Parched Power: Water Demands, Risks, and Opportunities for India's Power Sector," 2018.

[10] G. K. Sarangi, A. Mishra, Y. Chang, and F. Taghizadeh-Hesary, "Indian electricity sector, energy security and sustainability: An empirical assessment," *Energy Policy*, vol. 135, Dec. 2019, doi: 10.1016/j.enpol.2019.110964.

[11] C. J. Axon and R. C. Darton, "Sustainability and risk – a review of energy security," *Sustainable Production and Consumption*, vol. 27. Elsevier B.V., pp. 1195–1204, Jul. 01, 2021. doi: 10.1016/j.spc.2021.01.018.

[12] Internationa Energy Agency (IEA), "Electricity Market Report - July 2022," 2022. Accessed: Mar. 01, 2023. [Online]. Available: https://www.iea.org/reports/electricity-market-report-july-2022

[13] P. Ekins, T. Domenech, P. Drummond, R. Bleischwitz, N. Hughes, and L. Lotti, "The Circular Economy: What, Why, How and Where," 2019. Accessed: Mar. 01, 2023. [Online]. Available: https://discovery.ucl.ac.uk/id/eprint/10093965/1/Ekins-2019-Circular-Economy-What-Why-How-Where.pdf

[14] M. A. Habib and S. M. Zubair, "Second-Law-Based Thermodynamic Analysis OF Regenerative-Reheat Rrankine-Cycle Power Plants," *Energy*, vol. 17, no. 3, pp. 295–301, 1992, doi: https://doi.org/10.1016/0360-5442(92)90057-7.

[15] T. Xin, C. Xu, and Y. Yang, "A general and simple method for evaluating the performance of the modified steam Rankine cycle: Thermal cycle splitting analytical method," *Energy Convers Manag*, vol. 210, Apr. 2020, doi: 10.1016/j.enconman.2020.112712.

[16] S. O. Oyedepo *et al.*, "Thermodynamics analysis and performance optimization of a re-heat – Regenerative steam turbine power plant with feed water heaters," *Fuel*, vol. 280, Nov. 2020, doi: 10.1016/j.fuel.2020.118577.

[17] E. Hu, Y. P. Yang, A. Nishimura, F. Yilmaz, and A. Kouzani, "Solar thermal aided power generation," *Appl Energy*, vol. 87, no. 9, pp. 2881–2885, 2010, doi: 10.1016/j.apenergy.2009.10.025.

[18] T. Prosin, T. Pryor, C. Creagh, L. Amsbeck, and R. Buck, "Hybrid Solar and Coal-fired Steam Power Plant with Air Pre-heating Using a Centrifugal Solid Particle Receiver," in *Energy Procedia*, May 2015, vol. 69, pp. 1371–1381. doi: 10.1016/j.egypro.2015.03.134.

[19] C. N. Nsanzubuhoro, T. Bello-Ochende, and A. G. Malan, "Second law analysis of a fossil-geothermal hybrid power plant with thermodynamic optimization of geothermal preheater," *Heat Transfer*, vol. 49, no. 7, pp. 3997–4018, Nov. 2020, doi: 10.1002/htj.21692.

[20] J. Li *et al.*, "Safety and thermal efficiency performance assessment of solar aided coal-fired power plant based on turbine steam double re-heat," *Energy*, vol. 226, Jul. 2021, doi: 10.1016/j.energy.2021.120277.

[21] J. Ling-Chin, H. Bao, Z. Ma, W. Taylor, and A. Paul Roskilly, "State-of-the-Art Technologies on Low-Grade Heat Recovery and Utilization in Industry," in *Energy Conversion - Current Technologies and Future Trends*, IntechOpen, 2019. doi: 10.5772/intechopen.78701.

[22] Y. Lan, S. Wang, J. Lu, H. Zhai, and L. Mu, "Comparative analysis of organic rankine cycle, Kalina cycle and thermoelectric generator to recover waste heat based on energy, exergy, economic and environmental analysis method," *Energy Convers Manag*, vol. 273, Dec. 2022, doi: 10.1016/j.enconman.2022.116401.

[23] U. Larsen, F. Haglind, and O. Sigthorsson, "A comparison of advanced heat recovery power cycles in a combined cycle for large ships," in *Proceedings of ECOS 2013 - The 26th International Conference on Efficiency, Cost, Optimization, Simulation and Environmental Impact of Energy Systems*, 2013.

[24] M. N. Karimi, A. Dutta, A. Kaushik, H. Bansal, and S. Z. Haque, "A Review of Organic Rankine, Kalina and Goswami Cycle," *International Journal of Engineering Technology, Management and Applied Sciences*, vol. 3, 2015, [Online]. Available: https://www.researchgate.net/publication/283302991

[25] H. Chen, D. Y. Goswami, and E. K. Stefanakos, "A review of thermodynamic cycles and working fluids for the conversion of low-grade heat," *Renewable and Sustainable Energy Reviews*, vol. 14, no. 9, pp. 3059–3067, 2010, doi: 10.1016/j.rser.2010.07.006.

[26] C. Ballzus, H. Frimannson, G. I. Gunnarsson, and I. Hrolfsson, "The Geothermal Power Plant at Nesjavellir, Iceland," in *World Geothermal Congress*, 2000.

[27] V. Colucci, G. Manfrida, B. Mendecka, L. Talluri, and C. Zuffi, "LCA and Exergo-Environmental Evaluation of a Combined Heat and Power Double-Flash Geothermal Power Plant," *Sustainability (Switzerland)*, vol. 13, no. 4, pp. 1–23, Feb. 2021, doi: 10.3390/su13041935.

[28] Imasa Technologies S.L.U. (Imatec), "Hygroscopic Cycle." https://imasatechnologies.com/tecnologia-hct/ (accessed Mar. 01, 2023).

[29] F. J. Rubio-Serrano, F. Soto-Pérez, and A. J. Gutiérrez-Trashorras, "Experimental study on the influence of the saline concentration in the electrical performance of a Hygroscopic cycle," *Appl Therm Eng*, vol. 165, Jan. 2020, doi: 10.1016/j.applthermaleng.2019.114588.

[30] F. J. Rubio-Serrano, F. Soto-Pérez, and A. J. Gutiérrez-Trashorras, "Influence of cooling temperature increase in a hygroscopic cycle on the performance of the cooling equipment," *Energy Convers Manag*, vol. 200, Nov. 2019, doi: 10.1016/j.enconman.2019.112080.

[31] F. J. Rubio-Serrano, A. J. Gutiérrez-Trashorras, F. Soto-Pérez, E. Álvarez-Álvarez, and E. Blanco-Marigorta, "Advantages of Incorporating Hygroscopic Cycle Technology to a 12.5-MW Biomass Power Plant," *Appl Therm Eng*, vol. 131, pp. 320–327, Feb. 2018, doi: 10.1016/j.applthermaleng.2017.12.027.

[32] A. Meana-Fernández, B. Peris-Pérez, A. J. Gutiérrez-Trashorras, S. Rodríguez-Artime, J. C. Ríos-Fernández, and J. M. González-Caballín, "Optimization of the propulsion plant of a Liquefied Natural Gas transport ship," *Energy Convers Manag*, vol. 224, Nov. 2020, doi: 10.1016/j.enconman.2020.113398.

[33] A. Meana-Fernández, J. M. González-Caballín, R. Martínez-Pérez, F. J. Rubio-Serrano, and A. J. Gutiérrez-Trashorras, "Power Plant Cycles: Evolution towards More Sustainable and Environmentally Friendly Technologies," *Energies*, vol. 15, no. 23. MDPI, Dec. 01, 2022. doi: 10.3390/en15238982.

[34] F-Chart, "EES - Engineering Equation Solver. Version: V10.833-3D." [Online]. Available: https://fchartsoftware.com/ees/

[35] Z. Yuan and K. E. Herold, "Thermodynamic properties of aqueous lithium bromide using a multiproperty free energy correlation," *HVAC and R Research*, vol. 11, no. 3, pp. 377–393, 2005, doi: 10.1080/10789669.2005.10391144.

[36] Bombas Grundfos España S.A., "Centrifugal Pumps." https://www.grundfos.com/es (accessed Mar. 01, 2023).

[37] M. Shamoushaki, D. Fiaschi, G. Manfrida, and L. Talluri, "Energy, exergy, economic and environmental (4E) analyses of a geothermal power plant with NCGs reinjection," *Energy*, vol. 244, Apr. 2022, doi: 10.1016/j.energy.2021.122678.

[38] A. M. Blanco-Marigorta and J. D. Marcos, "Key issues on the exergetic analysis of H2O/LiBr absorption cooling systems," *Case Studies in Thermal Engineering*, vol. 28, Dec. 2021, doi: 10.1016/j.csite.2021.101568.

[39] R. Arjona, A. García, and P. Ollero, "The drying of alpeorujo, a waste product of the olive oil mill industry," *J Food Eng*, vol. 41, pp. 229–234, 1999, doi: 10.1016/S0260-8774(99)00104-1.

[40] M. Orive, B. Iñarra, M. Cebrián, and J. Zufía, "New integrated polyphenols recovery and anaerobic digestion of alpeorujo," in *3rd Edition of the International Conference on Wastes: Solutions, Treatments and Opportunities*, 2015. doi: 10.13140/RG.2.1.2059.3125.

[41] J. A. Alburquerque, J. Gonzálvez, D. García, and J. Cegarra, "Composting of a solid olive-mill by-product ('alperujo') and the potential of the resulting compost for cultivating pepper under commercial conditions," *Waste Management*, vol. 26, no. 6, pp. 620–626, 2006, doi: 10.1016/j.wasman.2005.04.008.